第 28 卷第 12 期 无 机 化 学 学 报 Vol.28 No.12
2012 年 12 月 CHINESE JOURNAL OF INORGANIC CHEMISTRY 2660-2666

甘氨酸辅助水热合成不同形貌的 CaF_2:Ln^{3+}(Ln=Eu, Tb)微米晶

王 森 沈新林 汤艳峰 江国庆 石玉军*
(南通大学化学化工学院,南通 226019)

摘要: 以 KBF_4 和 K_2SiF_6 作为氟源,采用简单的甘氨酸辅助水热法制得了一系列具有不同形貌的 CaF_2:Ln^{3+}(Ln=Eu,Tb)微米晶,如立方体、空心多面体和空心球。由 XRD、FTIR、SEM 及 PL 对产物的纯度、晶相、形貌和荧光性质进行了表征。XRD 结果显示所有产物均为结晶良好的立方相 CaF_2。SEM 结果表明,在添加甘氨酸的情况下,由 KBF_4 得到的产物为空心多面体结构,而由 K_2SiF_6 制得的产物是由许多纳米块自组装成的空心球。研究发现甘氨酸、氟源种类、时间等反应参数在不同形貌 CaF_2:Ln^{3+}(Ln=Eu,Tb)的形成过程中发挥关键作用,并提出了可能的反应机理。

关键词: CaF_2; 纳米材料; 水热法; 甘氨酸; 荧光
中图分类号: O614.23+1; O613.41 **文献标识码**: A **文章编号**: 1001-4861(2012)12-2660-07

Glycine-Assisted Hydrothermal Synthesis of CaF_2:Ln^{3+}(Ln=Eu, Tb) Microcrystals with Different Morphologies

WANG Miao SHEN Xin-Lin TANG Yan-Feng JIANG Guo-Qing SHI Yu-Jun*
(*School of Chemistry and Chemical Engineering, Nantong University, Nantong, Jiangsu* 226019, *China*)

Abstract: By employing KBF_4 or K_2SiF_6 as fluoride source, a facile glycine-assisted hydrothermal route has been developed to synthesize a series of well-dispersed CaF_2:Ln^{3+}(Ln=Eu, Tb) microcrystals with a variety of morphologies, such as cubes, hollow polyhedra and hollow spheres. X-ray diffraction (XRD), Fourier transform IR (FTIR), scanning electron microscopy (SEM) and photoluminescence (PL) were used to characterize the purity, crystalline phase, morphologies and the photoluminescence properties of the samples. The XRD results show that all the as-prepared CaF_2 have cubic structure and high crystallinity. The SEM results indicate that, in the presence of glycine, the as-prepared CaF_2 microcrystals present morphologies of highly dispersed hollow polyhedra and hollow spheres obtained from KBF_4 and K_2SiF_6, respectively. Meanwhile, the CaF_2 hollow spheres were assembled from numerous nanocubes. In the synthetic process, glycine, fluoride source and reaction time play crucial role in confining the growth of the different morphological CaF_2 microcrystals. The growth mechanism for products with diverse microstructures have been proposed based on the experimental results.

Key words: CaF_2; nanomaterials; hydrothermal route; glycine; photoluminescence

0 Introduction

Inorganic fluoride materials have diverse optical applications owing to their low energy phonons and high ionicity, which lead to less absolute fundamental absorption with respect to other oxide or sulfide

收稿日期:2012-03-27。收修改稿日期:2012-06-25。
国家自然科学基金(No.21173122,20906052),江苏省自然科学基金(No.BK2010281),南通市应用研究计划项目(BK2011035),南通大学校级课题(09ZY003;10ZY004)资助项目。
*通讯联系人。E-mail:wangmiao@ntu.edu.cn

materials[1]. As an important fluoride, CaF_2 has attracted increasing interest with res a nd biocompatible luminescent markers[2-4]. So far, dramatic efforts have been dedicated to the exploration of various convenient and efficient approaches for the fabrication of a range of CaF_2. To date, several kinds of wet chemical approaches have been developed to synthesize CaF_2 nano/microstructures, such as polyol method[4], solvothermal or hydrothermal methods[5-8], thermolysis[9-10], coprecipitation[11-12], solvent extraction route[13] and sonochemical route[14]. Correspondingly, a series of different morphological CaF_2 nano/microstructures have been fabricated, such as nanoparticles[4], cubes[5], plates & polyhedra & truncated octahedron[6-7,9-10], wires[11], hollow spheres[12-13] and flowers[8,14].

In recent years, the biomolecule-assisted routes have been widely used in the synthesis of complicated structures because of their special structures and fascinating self-assembling functions. Among them, the glycine-templated method may provide an alternative for controlling of inorganic crystal growth and fabricating novel micro/nanostructures. Up to now, a variety of inorganic micro/nanomaterials, such as LaF_3 nanoplates[15], YPO_4 bundles[16], Fe_2O_3 nanospheres[17] and 3D hierarchical $Zn_3(OH)_2V_2O_7\cdot 2H_2O$ microspheres[18] have been prepared via glycine-assisted route. However, to the best of our knowledge, few studies have focused on the synthesis of CaF_2 by glycine-assisted method. Herein, we present a simple glycine-assisted hydrothermal route to selectively synthesize different morphological CaF_2 microcrystals. It is found that the shapes and dimensions of the products are strongly dependent on the reaction condition, such as the amount of glycine, fluoride source and reaction time, only the optimum ratio of three factors is favorable for the formation of unique morphological products.

1 Experimental

1.1 Preparation

$CaCl_2$, KBF_4, K_2SiF_6 and glycine ($C_2H_5NO_2$) (AR) were purchased from Shanghai Chemical Reagent Corporation and used without further purification. Lanthanide oxides Ln_2O_3 (Ln=La, Eu, 99.99 %) and Tb_4O_7 (99.99%) were purchased from Shanghai Yue Long New Materials Corporation. In a typical process, 2 mmol of $CaCl_2$ and 2 mmol of glycine ($C_2H_5NO_2$) were added to 25 mL distilled water under stirring. When these reagents were dissolved, 1 mmol of KBF_4 was put into the solution. After stirring for 20 min, the obtained suspension was transferred into a 30 mL-teflonlined autoclave. The autoclave was sealed and heated at 120 ℃ for 12 h, then cooled to room temperature naturally. The white products were precipitated by centrifugation, washed with distilled water and ethanol, and finally dried at 70 ℃ for 4 h. 5% Ln^{3+}-doped CaF_2 were prepared using the same hydrothermal treatment as the undoped sample except that 0.1 mmol of $Ln(NO_3)_3\cdot 6H_2O$ (Ln=Eu, Tb) and 1.9 mmol of $CaCl_2$ were used instead of 2 mmol of $CaCl_2$.

1.2 Materials characterization

The FTIR spectrum was recorded between 4 000 and 400 cm^{-1} on a Nicolet AVATAR 370 instrument. The crystalline phases of the products were analyzed by XRD on a Bruker D8-Advance powder X-ray diffractometer (Cu $K\alpha$ radiation, λ=0.154 18 nm), employing a scanning rate of 4.00°·min^{-1}, in the 2θ range from 20° to 80°. The operation voltage and current were maintained at 40 kV and 40 mA, respectively. The sizes and morphologies of the resulting products were studied by field emission scanning electron microscopy (FE-SEM, HITACHI S-4800) at 15 kV. The luminescent spectra of the solid samples were recorded on HITACHI F-4500 spectro photometer at room temperature.

2 Results and discussion

2.1 Structure characterization

The XRD patterns for the sample in a typical experiment is shown in Fig.1a, with the fixed molar ratio of $CaCl_2$/Gly/KBF_4 at 2∶2∶1, all diffraction peaks can be indexed to cubic structured CaF_2 (PDF No. 04-0864). No peak of impurities is observed, confirming the formation of pure CaF_2. The strong and sharp diffraction peaks indicate that the as-obtained products

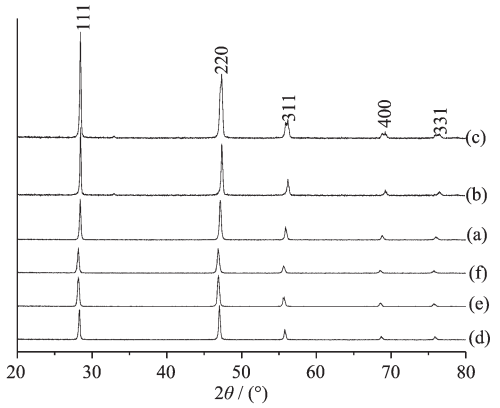

(a) n_{CaCl_2}:n_{Gly}:n_{KBF_4}=2:2:1, (b) n_{CaCl_2}:n_{Gly}:n_{KBF_4}=2:1:1, (c) n_{CaCl_2}:n_{Gly}:n_{KBF_4}=2:0:1, (d) n_{CaCl_2}:n_{Gly}:$n_{K_2SiF_6}$=2:0:1, (e) n_{CaCl_2}:n_{Gly}:$n_{K_2SiF_6}$=2:1:1, (f) n_{CaCl_2}:n_{Gly}:$n_{K_2SiF_6}$=2:2:1

Fig.1 XRD patterns of the product obtained after reaction for 12 h

are well-crystalline ones.

2.2 Morphology characterization

Fig.2a ~b show the SEM images of the products obtained in a typical procedure, when 2 mmol glycine is used. As shown in the low-magnification SEM image (Fig.2a), a large number of mono-dispersed polyhedra with the edge length about 50~100 nm are formed, no other morphologies can be detected. The product is of a similar shape with those reported truncated octahedron[7]. However, from the magnified SEM image (Fig.2b), it is found that there are a few holes on the surface of CaF_2 polyhedra, indicating the hollow nature of the polyhedra.

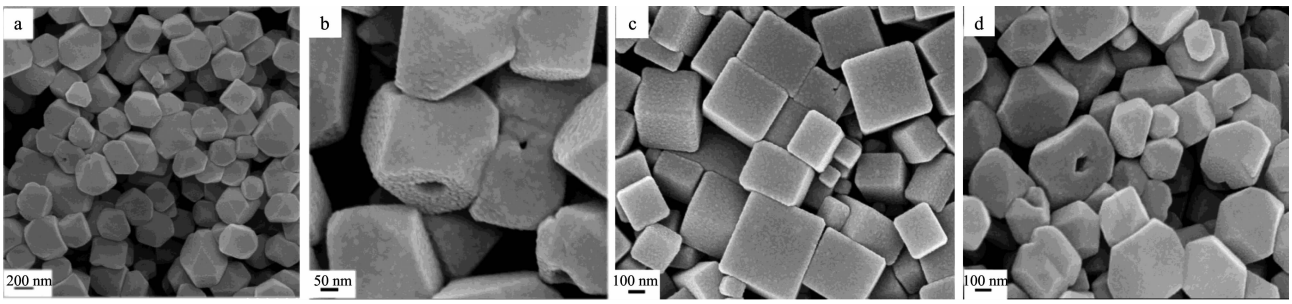

Fig.2 SEM images of the products prepared from KBF_4 with the molar ratio of $CaCl_2$/glycine/KBF_4 as 2:2:1 (a~b); 2:0:1 (c); 2:1:1 (d)

2.3 Effect of reaction parameters

To obtain a better understanding of the crystal growth procedure, controlled trials are performed to investigate the effect of glycine on the morphologies of the products. When KBF_4 is used as fluoride source, all diffraction peaks of the products obtained from different amounts of glycine can all be indexed to cubic phased CaF_2 (Fig.1b~c). Therefore, the molar ratio of Ca^{2+}/Gly/BF_4^- has no great effect on the crystalline phase. However, the diffraction peaks obtained from $CaCl_2$/Gly/KBF_4 as 2:0:1 are much sharper than the product obtained from 2:2:1. According to Scherrer equation, it is clearly indicated that with the increasing of glycine, the size of the products is decreased. The corresponding SEM images of as-prepared products are shown in Fig. 2c ~d. In the absence of glycine, it is found that the morphology of the as-prepared CaF_2 consists of highly dispersed cubes with edge length of 150~400 nm (Fig. 2c). The size of the cubes is different from each other. This observation indicates that glycine plays a key role in controlling the morphology and size of the products. When 1 mmol glycine is added, irregular polyhedra coexisted holes are formed (Fig.2d). These results indicate that the morphologies of the CaF_2 microstructures are sensitive to the amount of glycine.

In order to investigate the effect of fluoride source, another complex fluoride, K_2SiF_6 is used instead of KBF_4 to synthesize CaF_2 by an identical procedure. As shown in Fig.1d ~f, the products obtained from K_2SiF_6 can also be characterized as pure cubic phased CaF_2 (PDF No. 04-0864). However, the diffraction peaks obtained from $CaCl_2$/glycine/K_2SiF_6 as 2:0:1 (Fig.1d) are much sharper than those of the product obtained from 2:2:1 (Fig.1e). The SEM images of the product obtained from different molar ratios of $CaCl_2$/glycine/K_2SiF_6 are shown in Fig.3a~e. When the molar ratio is fixed as 2:0:1, namely, in the absence of glycine, the morphology of the as-prepared CaF_2 consists of irregular polyhedra

(Fig.3a). These results are well agreeable with those reported[14]. When 1 mmol glycine is added, the as-prepared CaF_2 are small irregular cubes with different sizes (Fig.3b~c), and many of the cubes are aggregated together. When the amount of glycine is increased to 2 mmol, homogeneous cage-like hollow spheres with diameters of about 500 nm were formed, as shown in Fig.3d. The magnified SEM images (Fig.3e) indicate that the hollow microspheres are constructed by many cubes with the diameter of 100 nm. It is worthy to note that there are a great number of different sized pores on the coarse surfaces of microspheres. Consequently, with increase of the glycine, the CaF_2 hollow microspheres undergo a self-assemble process in the morphological evolution from nanocubes. The above results also reveal that the fluoride sources have remarkable impacts on the morphologies of the as-prepared CaF_2.

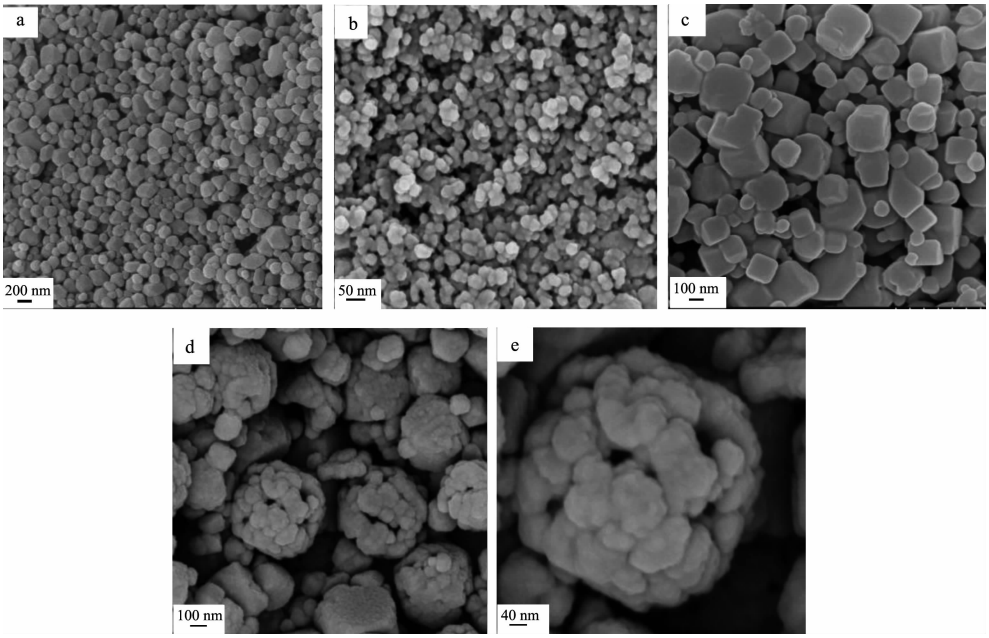

Fig.3　SEM images of the products prepared from K_2SiF_6 with the molar ratio of $CaCl_2$/glycine/K_2SiF_6 as 2:0:1 (a); 2:1:1 (b~c) and 2:2:1 (d~e)

Furthermore, a series of time-dependent experiments were carried out to investigate the growth details. Fig.4a~b are the SEM images of the products after 6 h and 24 h of reaction time, respectively, when the molar ratio of $CaCl_2$/glycine/KBF_4 is fixed as 2:2:1. The morphologies of the CaF_2 obtained from 6 h are monodispersed polyhedra (Fig.4a). When the reaction time is increased to 24 h, a large number of irregular polyhedron is formed. Of particular interest is that some of these polyhedra are hollow inside, which is similar to that obtained in 12 h (Fig.2b). When K_2SiF_6 is employed as the fluoride source, and the molar ratio of $CaCl_2$/glycine/K_2SiF_6 is fixed at 2:2:1, after 6 h, the SEM image in (Fig.4c) shows that the product is composed of

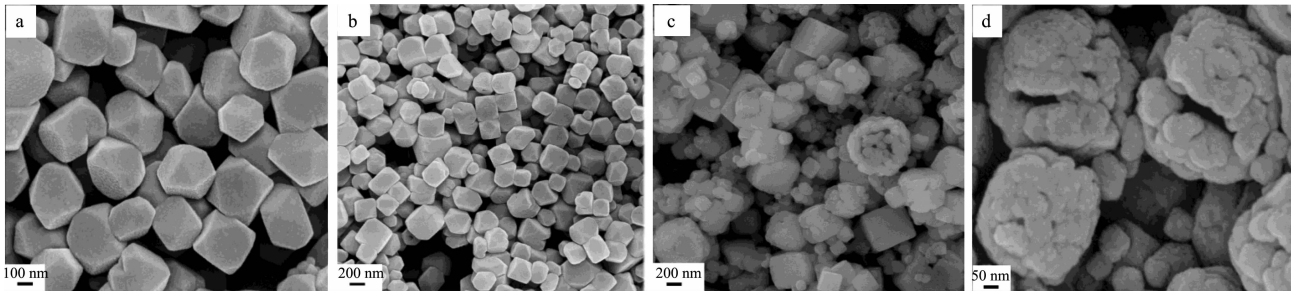

(a) 6 h and (b) 24 h when molar ratio of $CaCl_2$/glycine/KBF_4 as 2:2:1; (c) 6 h and (d) 24 h when molar ratio of $CaCl_2$/glycine/K_2SiF_6 as 2:2:1

Fig.4　SEM images of the products prepared from KBF_4 or K_2SiF_6 within different reaction times

a majority of cagelike aggregates assembled by nanocubes, accompanying a small fraction of microcubes. After 24 h, many hollow microspheres are obtained. The surface of the spheres is rough and composed of small nanocubes. Therefore, the morphologies of the product are time-dependent. In addition, the concentration of the starting materials has not influence on the crystalline phases of the products. For instance, a reaction using the molar ratio of Ca^{2+}/BF_4^- as 1:0.5 gives CaF_2 with the same crystalline phase and morphology, but the yield is much lower.

2.4 Possible formation mechanism

As shown in Fig.5a, there are clear displacements for some of the main absorption peaks of the Ca-gly complex compared with the pure glycine. Located in 3 169 cm^{-1} of the characteristic absorption peak for glycine is disappeared after the Ca-gly complex formed. The peaks at 1 407 and 1 589 cm^{-1} can be assigned to the symmetric stretching vibration and antisymmetric stretching vibration of $-COO^-$ in Ca-gly complex. However, they should be located in 1413 and 1612 cm^{-1} in pure glycine. Therefore, the groups $-NH_2$ and -COOH in glycine are all coordinated with Ca^{2+}. These data are consistent with the previous reports[19-20]. The formation of Ca-gly complex are further affirmed by XRD. As shown in Fig.5b, the position and the intensity of the diffraction peaks for Ca-gly complex are of great differences from the the pure glycine. The strong diffraction peaks indicate that the as-obtained products are new materials instead of the mixture of Ca-gly complex and glycine.

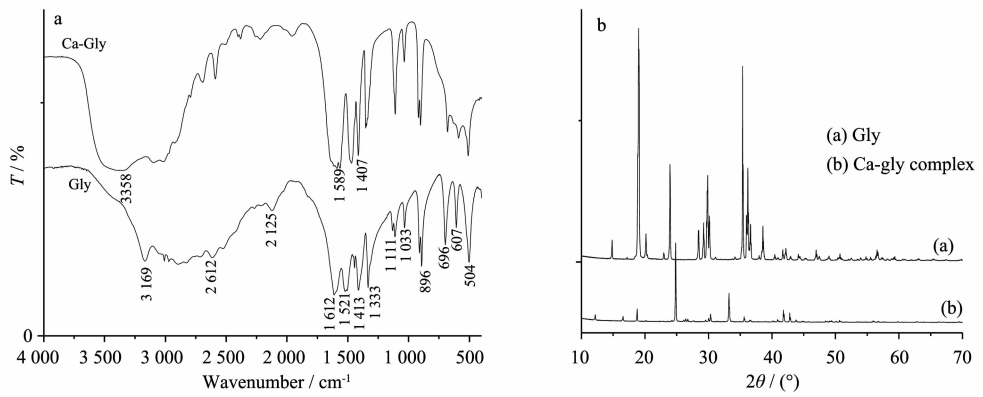

Fig.5 FTIR (a) and XRD (b) patterns of pure glycine and Ca-gly complex (molar ratio as 2:1)

From above experimental results, a possible growth mechanism based on self-assembly and Ostwald-ripening processes is proposed (Fig.6). It is known that KBF_4 (or K_2SiF_6) yields F by hydrolysis of BF_4(or SiF_6^{2-}). In the current study, Ca^{2+} and glycine formed complexes at the beginning. The F^- ions are first released from KBF_4 (or K_2SiF_6) and then react with the Ca^{2+} ions (released from the Ca-Gly complex) to form CaF_2 nanoparticles. Once the CaF_2 nanoparticles formed, the decomposed products from KBF_4 (or K_2SiF_6) can selectively adsorbed onto certain crystallographic planes of the CaF_2 seeds. In a further crystallization process, as the growth rates of different crystal facets are unequal (i.e., anisotropic growth), leading to the preferential growth of some specific crystalline planes[14,18,21]. In the following stage, with the help of glycine molecules and the increasing of reaction time, the particles recrystallize, aggregate and oriente to minimize the surface energy. Such self-assembly and oriented attachment mechanisms have been revealed in the formation of several hollow structures. Therefore, it can be assumed that the glycine molecules, as a

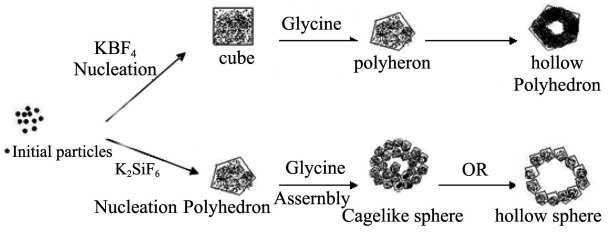

Fig.6 Schematic illustration for the formation mechanism of different morphological products

structure directing agent, facilitate the oriented growth and self-aggregation through the interactions between Ca^{2+} and -COOH (or -NH_2). Similar process has occurred in the system when EDTA or CTAB is used [14,18,21-23].

2.5 Photoluminescent properties

The emission spectra for 5mol% Eu^{3+} or Tb^{3+}-doped CaF_2 samples are shown in Fig.7. For Eu^{3+}-doped CaF_2, when the samples are excited at 395 nm, the corresponding emission peaks are observed at 591 nm, 613 nm, 648 nm and 684 nm. They originate from the transitions between the $^5D_0$ excited-state and the ^7F_J (J= 1, 2, 3, 4) ground states of Eu^{3+} ion[23]. Meanwhile, for Tb^{3+}-doped CaF_2, when the samples are excited at 376 nm, the emission spectrum exhibits four well-resolved peaks centered at 490, 543, 584, and 619 nm, corresponding to Tb^{3+} transitions of $^5D_4 \rightarrow {}^7F_J$ (where J=6, 5, 4, 3)[23]. As shown in Fig.7, although the major peaks in the emission spectra of these samples are identical, but the intensity is different. Yan and co-workers[24-25] have investigated the luminescent properties of rare earth doped nanomaterials and found that the emission intensity is size-dependent. They suggested that as the particle size of nanomaterials became smaller, the lattice become more distorted, which was responsible for the difference of the intensity patterns. The degree of crystallinity and the level of disorder are the other two factors affecting the luminescent properties of nanomaterials. It is generally believed that the morphology and the crystal structure should influence the luminescent properties of nanostructured particles. Therefore, the difference in luminescent properties of the products can be ascribed to the combined roles of their various dimensions, morphology, and the degree of crystallinity and crystalline phase. The reasons for these differences are not clear yet.

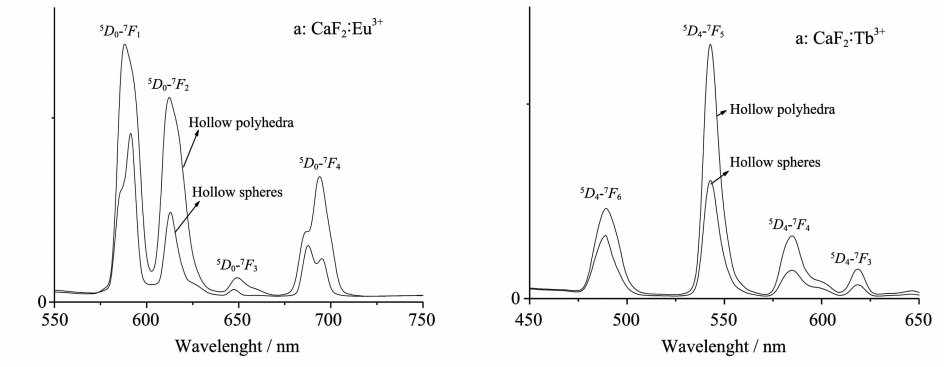

Fig.7　PL spectra of the 5% Eu^{3+}-doped CaF_2 (a) and Tb^{3+}-doped CaF_2 (b)

3 Conclusions

Via a simple hydrothermal route, cubic phased CaF_2 microcrystals with different morphologies (cubes, hollow polyhedra and hollow spheres) have been selectively synthesized. The glycine, fluoride sources and reaction time are key factors in the formation of different morphological CaF_2.

References:

[1] Nakajima T, Zemva B, Tressaud A. *Advanced Inorganic Fluorides*. Amsterdam: Elsevier, **2000**.

[2] Kinsman B E, Hanney R. *Adv. Mater. Opt. Electron.*, **1995**,**5**:109-115

[3] Moon H J, Kim K N, Kim K M, et al. *J. Biomed. Mater. Res. Part A*, **2005**,**74**A:497-502

[4] Feldmann C, Roming M, Trampert K. *Small*, **2006**,**2**:1248-1250

[5] Sun X M, Li Y D. *Chem. Commun.*, **2003**:1768-1769

[6] Zhang C M, Li C X, Peng C, et al. *Chem. Eur. J.*, **2010**,**16**: 5672-5680

[7] Zhang X M, Quan Z W, Yang J, et al. *Nanotechnology*, **2008**,**19**:075603(8pp)

[8] Hou S Y, Zou Y C, Liu X C, et al. *CrystEngComm*, **2011**,**13**:835-840

[9] Quan Z W, Yang D M, Yang P P, et al. *Inorg. Chem.*, **2008**,**47**:9509-9517

[10]Du Y P, Sun X, Zhang Y W, et al. *Cryst. Growth Des.*,

2009,**9**:2013-2019

[11]Mao Y B, Zhang F, Wong S S. *Adv. Mater.*, **2006**,**18**:1895-1899

[12]Wang W S, Zhen L, Xu C Y, et al. *ACS Appl. Mater. Interfaces*, **2009**,**1**:780-788

[13]Guo F Q, Zhang Z F, Li H F, et al. *Chem. Commun.*, **2010**, **46**:8237-8239

[14]WANG Miao(王淼), CHEN Ting-Ting(陈婷婷), TANG Yan-Feng(汤艳峰), et al. *Chinese J. Inorg. Chem.*(*Wuji Huaxue Xuebao*), **2012**,**28**:185-190

[15]Yang X F, Dong X T, Wang J X, et al. *J. Alloy Compd.*, **2009**,**487**:298-303

[16]Yang X F, Dong X T, Wang J X, et al. *Mater. Lett.*, **2009**, **63**:629-631

[17]Chen H M, Zhao Y Q, He J H, et al. *Analytica Chimica Acta*, **2010**,**659**:266-273

[18]Wang M, Shi Y J, Jiang G Q. *Mater. Res. Bull.*, **2012**,**47**: 18-23

[19]CHEN Guang-De(陈广德), XU Zhen-Mei(徐贞梅). *Fine Chem.*(*Jingxi Huagong*), **2002**,**19**:701-702,726

[20]ZHANG Da-Fei(张大飞), ZHAO Ri-Getu(照日格图), LIU Jian-Hua(刘建华), et al. *Chinese J. Spect. Lab.*(*Guangpu Shiyanshi*), **2006**,**23**:91-95

[21]CAO Xiao-Feng(曹霄峰), ZHANG Lei(张雷), MA Ying-Li(马英丽),et al. *Chinese J. Inorg. Chem.*(*Wuji Huaxue Xuebao*), **2010**,**26**:787-792

[22]Qian H S, Yu S H, Gong J Y, et al. *Cryst. Growth Des.* **2005**,**5**:935-939

[23]WANG Miao(王淼), SHI Yu-Jun(石玉军), JIANG Guo-Qing(江国庆). *Chinese J. Inorg. Chem.*(*Wuji Huaxue Xuebao*), **2009**,**25**:1785-1790

[24]Wei Z G, Sun L D, Jiang X C, et al. *Chem. Mater.*, **2003**,**15**: 3011-3017

[25]Jiang X C, Sun L D, Yan C H. *J. Phys. Chem. B*, **2004**,**108**: 3387-3390